PHYSICAL REVIEW D VOLUME 25, NUMBER 9 1 MAY 1982

Inclusive strange-resonance production in pp, π^+p, and K^+p interactions at 147 GeV/c

D. Brick, H. Rudnicka, A. M. Shapiro, and M. Widgoff
Brown University, Providence, Rhode Island 02912

R. E. Ansorge, J. R. Carter, W. W. Neale, J. G. Rushbrooke, D. R. Ward, and B. M. Whyman
University of Cambridge, Cambridge, England

R. A. Burnstein and H. A. Rubin
Illinois Institute of Technology, Chicago, Illinois 60616

J. W. Cooper, R. L. Plumer,* R. D. Sard, and J. O. Tortora[†]
University of Illinois, Urbana, Illinois 61801

E. D. Alyea
Indiana University, Bloomington, Indiana 47401

L. Bachman,[‡] C. -Y. Chien, and A. Pevsner
Johns Hopkins University, Baltimore, Maryland 21218

J. E. Brau,[§] E. S. Hafen, D. Hochman,[||] R. I. Hulsizer,
V. Kistiakowsky, P. Lutz,[¶] A. Napier,[**] I. A. Pless, J. P. Silverman,[††] P. C. Trepagnier, and R. K. Yamamoto
Laboratory for Nuclear Science and Department of Physics,
Massachusetts Institute of Technology, Cambridge, Massachusetts 02139

F. Grard, J. Hanton, V. Henri, P. Herquet, J. M. Lesceux, and R. Windmolders
Universite de l'Etat, Mons, Belgium

F. Crijns, H. deBock, W. Kittel, W. Metzger, C. Pols, M. Schouten, and R. Van de Walle
University of Nijmegen, Nijmegen, The Netherlands

H. O. Cohn
Oak Ridge National Laboratory, Oak Ridge, Tennessee 37830

G. Bressi, E. Calligarich, F. Carminati, C. Castoldi, R. Dolfini, and S. Ratti
University of Pavia and Instituto Nazionale Fisica Nucleare Pavia, Italy

R. DiMarco, P. F. Jacques, M. Kalelkar, R. J. Plano, P. Stamer,[‡‡] and T. L. Watts
Rutgers University, New Brunswick, New Jersey 08903

E. B. Brucker, E. L. Koller, and S. Taylor
Stevens Institute of Technology, Hoboken, New Jersey 08903

L. Berny, S. Dado, J. Goldberg, and S. Toaff
Technion, Haifa, Israel

G. Alexander, O. Benary, J. Grunhaus, and A. Levy
Tel-Aviv University, Ramat-Aviv, Israel

W. M. Bugg, G. T. Condo, T. Handler, and E. L. Hart
University of Tennessee, Knoxville, Tennessee 37916

Y. Eisenberg, U. Karshon, E. E. Ronat, A. Shapira, R. Yaari, and G. Yekutieli
Weizmann Institute of Science, Rehovot, Israel

D. A. Ljung,[§§] T. W. Ludlam,[||||] and H. D. Taft
Yale University, New Haven, Connecticut 06520

(Received 28 July 1981)

We have studied the inclusive production of $K^{*\pm}(890)$ and $Y^{*\pm}(1385)$ in pp, π^+p, and K^+p interactions at 147 GeV/c. The experiment used the Fermilab 30-inch hydrogen bubble chamber with the hybrid spectrometer system. Results are based on a sample of 1916 observed K_S and 932 observed Λ. Inclusive cross sections are given for $K^{*\pm}$ and $Y^{*\pm}$ production from the three beams, and comparisons are made with experiments at other energies. Feynman-x and transverse-momentum-squared distributions are also calculated. The results suggest that the K^{*-} is entirely produced in the central region, while the K^{*+} includes a component from beam fragmentation. Comparisons are made with the additive quark model.

I. INTRODUCTION

Recent studies of inclusive particle production in hadronic interactions have revealed that meson and baryon resonances are a major source of the final-state stable hadrons.[1] If the resonances are produced directly, their Feynman-x and $p_T{}^2$ distributions should reflect the underlying production dynamics more fundamentally than the corresponding distributions for the stable particles. Therefore the study of resonance production is crucial for an understanding of the nature of multiparticle production.

In this paper we report final results on inclusive $K^{*\pm}(890)$ and $Y^{*\pm}(1385)$ production in pp, π^+p, and K^+p interactions at 147 GeV/c, all in the same experiment. The reactions we have studied are

$$p+p\rightarrow K^{*+}(890)+\text{ anything}\,, \tag{1}$$

$$p+p\rightarrow K^{*-}(890)+\text{ anything}\,, \tag{2}$$

$$\pi^++p\rightarrow K^{*+}(890)+\text{ anything}\,, \tag{3}$$

$$\pi^++p\rightarrow K^{*-}(890)+\text{ anything}\,, \tag{4}$$

$$K^++p\rightarrow K^{*+}(890)+\text{ anything}\,, \tag{5}$$

$$K^++p\rightarrow K^{*-}(890)+\text{ anything}\,, \tag{6}$$

$$p+p\rightarrow Y^{*+}(1385)+\text{ anything}\,, \tag{7}$$

$$p+p\rightarrow Y^{*-}(1385)+\text{ anything}\,, \tag{8}$$

$$\pi^++p\rightarrow Y^{*+}(1385)+\text{ anything}\,, \tag{9}$$

$$\pi^++p\rightarrow Y^{*-}(1385)+\text{ anything}\,, \tag{10}$$

$$K^++p\rightarrow Y^{*+}(1385)+\text{ anything}\,, \tag{11}$$

$$K^++p\rightarrow Y^{*-}(1385)+\text{ anything}\,. \tag{12}$$

Previous experiments on inclusive resonance production have mainly focused on the nonstrange resonances such as the ρ^0 and Δ^{++}. There are only a few high-energy results on the K^* and Y^*. Above 16 GeV/c, strange-resonance production has been studied in pp collisions at 24 GeV/c (Ref. 2,3), 205 GeV/c (Ref. 4), 300 GeV/c (Ref. 5), and 405 GeV/c (Refs. 6,7). In π^+p interactions, the only results are at 16 GeV/c (Ref. 2) and 32 GeV/c (Ref. 8). Finally, in K^+p interactions, there is only one experiment,[9] at 32 GeV/c, reporting data on K^* production. In this paper we make comparisons between our results and those of previous experiments.

A number of theoretical models have addressed the subject of inclusive particle production, especially focusing on cross-section ratios for the production of stable as well as resonance states. In this paper we compare our results with an additive quark model[10] and with one based on multiperipheral ideas.[11] In making these comparisons we also use previously published[12,13] results from this experiment.

In Sec. II of this paper we discuss the experimental apparatus, the scanning, measuring, and reconstruction procedure, and the event-selection criteria. In Sec. III we give total inclusive cross sections for K^* production in reactions (1)–(6). In Sec. IV we present inclusive distributions for reactions (1)–(4). We show the dependence of the cross section on the Feynman scaling variable

$x=2P_L^*/\sqrt{s}$, where P_L^* is the longitudinal momentum of the K^* in the center of mass, and $\sqrt{s}$ is the total center-of-mass energy (about 16.6 GeV). We also present transverse-momentum-squared distributions and their slopes.

In Sec. V of this paper we give our results on inclusive $Y^*(1385)$ production in reactions (7)—(12). For some of these reactions we do not observe a significant signal, and therefore quote upper limits on the production cross sections.

II. EXPERIMENTAL PROCEDURE

The experiment (E299) was performed in the Fermilab 30-inch hydrogen bubble chamber with proportional wire chambers (PWC's) located both upstream and downstream. Details of this hybrid spectrometer system have been previously published.[14,15] Briefly, the upstream PWC's and a differential Čerenkov counter allowed tagging of π^+, K^+, and p in the incident beam. The downstream PWC's were used for momentum measurements of fast, forward particles from the primary vertex of an event. The downstream system also included a lead-glass forward γ detector. The magnetic field was 25 kG at the center of the bubble chamber.

The beam consisted of 147-GeV/c positive particles. A total of 400 000 pictures was taken in two runs, with different beam ratios in each. The final sample had an overall composition of 51% π^+, 9% K^+, and 40% p.

The film was scanned for all beam track interactions, and the vertices of primary events and vees were digitized by scanners. These predigitized events were subsequently measured on a Precision Encoding and Pattern Recognition (PEPR) machine in a semiautomatic mode. The program GEOHYB was used to perform view-to-view track matching and space reconstruction, as well as correlation of bubble-chamber and PWC information to obtain final track momenta.

For a vee to be accepted, its decay length had to exceed 2 cm in space from the primary vertex. In addition a decay volume was defined in such a way as to maximize the volume visible in all three views of the chamber. This volume was bounded by ten planes, two of which were parallel to the front and back glass surfaces but displaced 5 cm into the chamber in order to provide adequate length for decay track measurement. The scan efficiency for finding neutrals was determined to be (91 ± 3)% by doing a second scan on a fraction of the film.

Kinematic fitting of the vees to the primary vertex was accomplished with the program SQUAW. For each vee, three-constraint (3C) and (1C) fits were attempted corresponding to the following hypotheses:

$$K_S\rightarrow\pi^+\pi^- ,$$

$$\Lambda\rightarrow p\pi^- ,$$

$$\bar{\Lambda}\rightarrow\bar{p}\pi^+ ,$$

$$\gamma(p)\rightarrow(p)e^+e^- .$$

All vees making a 3C fit with a probability greater than 0.1% were accepted into the data sample. Vees that failed the 3C fit, but made a 1C fit with a probability over 0.1%, were also accepted if the angular difference between the measured and fitted neutral direction was less than 60 mrad. These 1C fits comprised only about 10% of the total, and their inclusion did not appreciably affect any of the results presented in this paper.

A total of 6744 vees constituted the final data sample, of which about 18% had ambiguous fits. Some of these ambiguities were easy to resolve, because the relative probabilities for the competing fits differed by a factor of 10 or more. In these cases the more probable fit was selected. 3C fits were also given priority over competing 1C fits. About 11% of the vees remained ambiguous after this step, and a more elaborate procedure was used for them.

(a) If the ambiguity included a γ fit, we examined the transverse momentum of the negative decay track with respect to the line of flight of the neutral decaying track. This is a useful quantity because for strange particles its spectrum is sharply peaked at the kinematic maximum, while for γ conversions it is peaked at zero. Thus this quantity provides a clean separation of strange-particle fits ambiguous with γ's. If the transverse momentum of the negative decay track was less than 40 MeV/c, the neutral was assigned to the γ sample; otherwise, the competing strange-particle fit was chosen.

(b) Ambiguities involving only strange-particle fits were resolved by examining distributions of $\cos\theta^*$, where θ^* is the angle between the neutral line of flight and the direction of the negative decay product in the rest frame of the neutral. This distribution must be isotropic for the spin-zero K, and also isotropic for the Λ and $\bar{\Lambda}$ if they are produced with no longitudinal polarization. Selections were made on relative fit probabilities in such a way as to render these decay angular distributions

roughly isotropic. Specifically, an ambiguous vee was selected as a K_S only if its probability as a K_S was more than 40% greater than the probability for Λ as well as $\bar{\Lambda}$. Ambiguities between Λ and $\bar{\Lambda}$ were resolved by using the higher probability fit.

This procedure resulted in a final sample of 1916 K_S's, 932 Λ's, 164 $\bar{\Lambda}$'s, and 3732 γ's. Figure 1 shows the decay angular distributions for the K_S and Λ; it is apparent that these are approximately isotropic, so that the allocation of ambiguities is reasonable at least on a statistical basis. Table I summarizes the number of vees of each type obtained from each of the three beams.

A measure of the experimental resolution is provided in Figs. 2 and 3, which show the unconstrained effective-mass distributions for the K_S and Λ, respectively, in the final event sample. When fitted to a Gaussian, the K_S plot has a σ of 4.9 MeV, while the Λ has a σ less than 1.8 MeV.

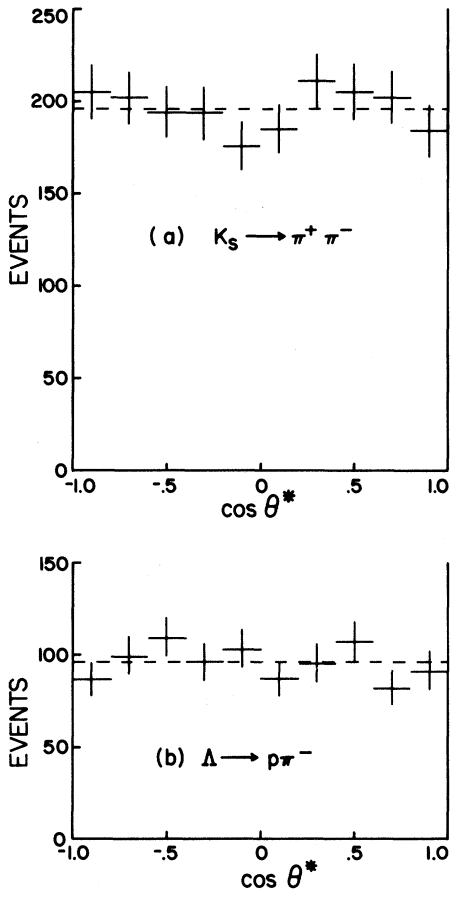

FIG. 1. Center-of-mass decay angular distributions for (a) K_S and (b) Λ. The dashed line indicates the average number of events in each bin. The distributions are expected to be isotropic.

III. INCLUSIVE $K^{*\pm}(890)$ CROSS SECTIONS

In order to calculate inclusive cross sections for $K^{*\pm}(890)$ production in reactions (1)—(6), we first weighted each observed K_S to correct for detection inefficiency due to the imposition of the minimum length cut and decay volume restriction. The average escape weight was 1.98 for K_S. We then made a weighted $K_S\pi^\pm$ effective-mass distribution for K_S events from all three beams. All outgoing particles from the primary event vertex were assumed to be pions, except for those (below 1.4 GeV/c) which were identified as protons from ionization. The resulting distribution is shown in Fig. 4. A clear peak is apparent in the vicinity of the $K^*(890)$.

We next performed a fit to the mass distribution, using a smooth polynomial background and a simple Breit-Wigner shape for the resonance. The mass and width of the resonance were allowed to vary in the fitting procedure. The best fit, which had a χ^2 of 1.4 per degree of freedom, yielded a mass of 888 ± 5 MeV and a width of 40 ± 10 MeV for the K^*. These numbers are entirely consistent with the world-average values[16] for the $K^*(890)$ parameters, so that we conclude that we are indeed observing this resonance. For all subsequent fits to the K^* reported in this paper, we fixed the mass at 888 MeV and the width at the world-average value of 50 MeV.

Escape-weighted mass distributions for $K_S\pi^+$ and $K_S\pi^-$ from the proton beam are shown in Figs. 5(a) and 5(b), respectively, while the corresponding distributions for the π^+ beam are shown in Figs. 6(a) and 6(b). Fits to these distributions were performed as described above, and yielded the numbers of resonant events in each channel. To determine the inclusive cross sections, the numbers of escape-weighted events were corrected to account for scan inefficiency, measurement and geometrical-reconstruction losses, and neutral decay modes of the K_S. A further weight of 2.0 was applied to include the contribution from K_L, and finally the

TABLE I. Number of K_S, Λ, $\bar{\Lambda}$, and γ for each beam type.

	p beam	π^+ beam	K^+ beam
K_S	882	912	122
Λ	464	414	54
$\bar{\Lambda}$	63	91	10
γ	1732	1755	245

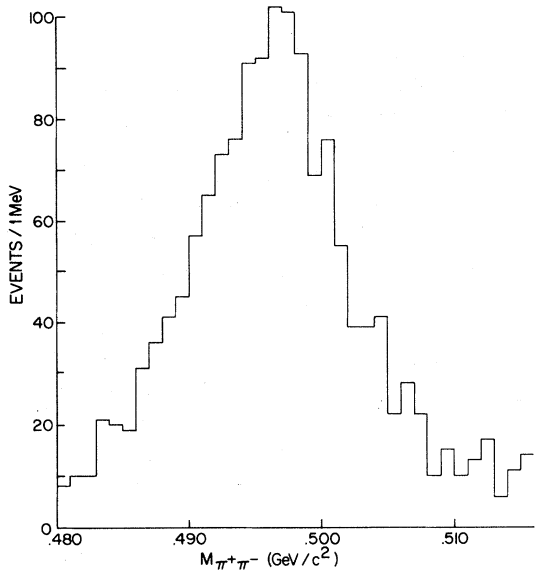

FIG. 2. The unconstrained effective-mass distribution of the decay prongs of vees accepted into the K_S sample.

branching ratio of $\frac{2}{3}$ for $K^{*\pm} \to K^0\pi^\pm$ was incorporated.

To determine the error in the inclusive cross sections, we included the statistical uncertainty, the uncertainty in each of the corrections made (such as scan efficiency), and the uncertainty in the Breit-Wigner fitting procedure. The error in the fit parameters was determined by noting the variation in parameter values that increased the χ^2 by one.

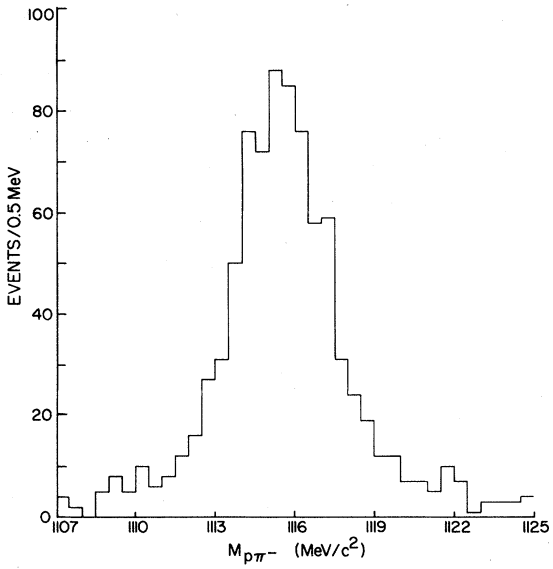

FIG. 3. The unconstrained effective-mass distribution of the decay prongs of vees accepted into the Λ sample.

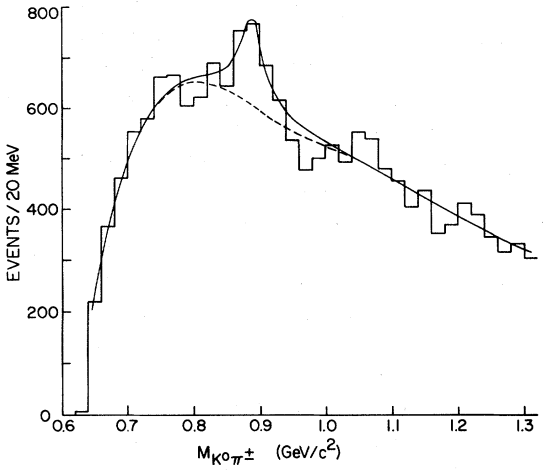

FIG. 4. Sum of $K^0\pi^+$ and $K^0\pi^-$ effective-mass distributions from all three beams. The events are weighted for geometric detection efficiency. The solid line represents a fit to the data using a Breit-Wigner shape for the K^*. The dashed line indicates the background.

Table II summarizes the inclusive cross sections for K^{*+} and K^{*-} production in reactions (1)–(6). It may be observed that for the proton beam the cross sections for the two charge states of the K^*

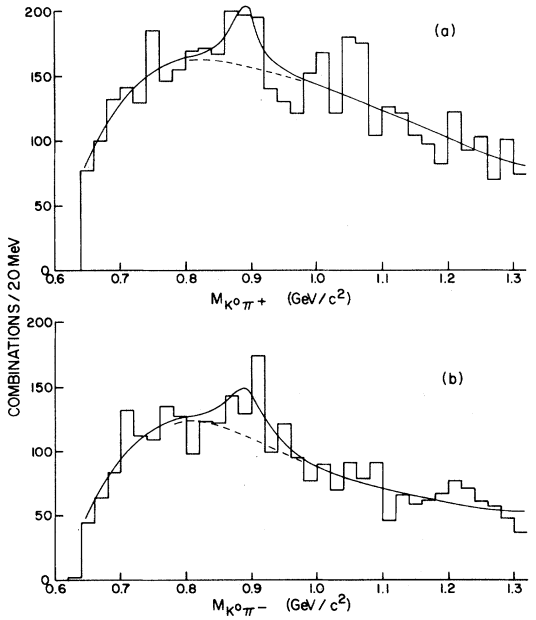

FIG. 5. Escape-weighted effective-mass distributions of (a) $K^0\pi^+$ and (b) $K^0\pi^-$ for events from the proton beam. The solid line represents a Breit-Wigner fit, while the dashed line indicates the background.

are approximately equal, although there is an indication of a slight excess of K^{*+} over K^{*-}. For the meson beams there is good evidence that the K^{*+} cross section exceeds the K^{*-} cross section, suggesting that a portion of the K^{*+} production occurs in the beam fragmentation region. We will return to this point in Sec. IV.

We have added the K^{*+} and K^{*-} cross sections for each beam, and in Fig. 7 we display the total $K^{*\pm}$ cross section as a function of incident beam momentum, using data from other experiments[2–9] as well as our own. It is readily apparent that for the proton beam the $K^{*\pm}$ cross section is rising sharply with energy. A rise is also suggested for the π^+ beam, although here the conclusion is less firm since there are only two measurements besides our own. For the K^+ beam, our value is about the same as that of an experiment, at much lower momentum (32 GeV/c). However, it should be noted that a very fast K^0, originating from a leading K^{*+}, is likely to decay outside the bubble chamber. It is likely, therefore, that this systematic problem results in an underestimate of the K^{*+} cross section from the K^+ beam. This conclusion is supported by new results from a 70-GeV/c K^+p experiment[17] using a larger bubble chamber than ours, with greater geometric detection efficiency. This experiment measures a K^{*+} cross section of 4.1 ± 0.3 mb, which is somewhat higher than our value.

We have studied this systematic bias against the detection of a fast, forward K^0 to see what effects it has on our results. One approach we have used is to look at Λ production in pp interactions, where the forward and backward regions must necessarily be symmetric. We find[12] that our escape-weighting procedure does yield the requisite symmetry out to about $|x|=0.4$. Beyond this value, we find that the forward Λ begin to get depleted relative to the backward Λ.

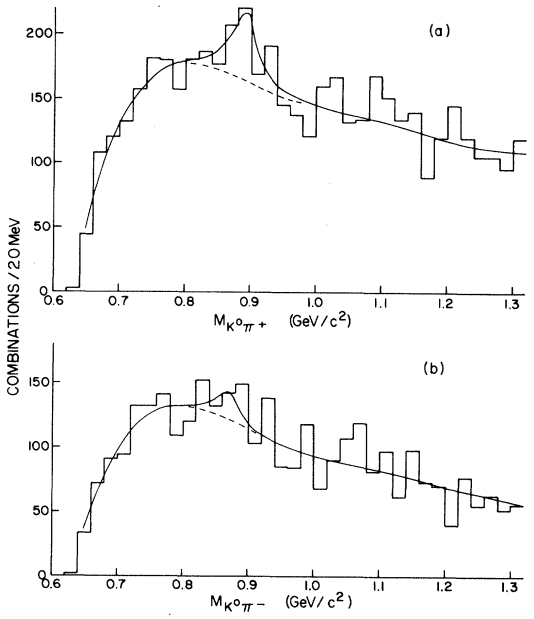

FIG. 6. Escape-weighted effective-mass distributions of (a) $K^0\pi^+$ and (b) $K^0\pi^-$ for events from the π^+ beam. The solid line represents a Breit-Wigner fit, while the dashed line indicates the background.

In the case of the K^*, we find that there is very little production in the extreme backward region, so that the systematic bias does not affect our results significantly. For example, in Table II we give the total K^* cross sections that we observe in pp interactions. If we take only the cross section in the backward hemisphere, and then double it, we obtain 1.8 ± 0.4 mb and (1.2 ± 0.4) mb for the K^{*+} and K^{*-}, respectively. These values are entirely consistent with the ones in Table II.

In Table II we also give the ratio of the charged K^* cross section to the cross section for $(K^0+\bar{K}^0)$ production. If it is assumed that $\sigma(K^{*0}+\bar{K}^{*0})$ is equal to $\sigma(K^{*+}+K^{*-})$, it turns out that the cross-section ratio $\sigma(K^{*+}+K^{*-})/\sigma(K^0+\bar{K}^0)$ is

TABLE II. Inclusive cross sections for K^{*+} and K^{*-} production. The cross sections are corrected for all unobserved decay modes.

Reaction	σ (mb)	$\sigma(K^*)/\sigma(K^0+\bar{K}^0)$
$pp\to K^{*+}+$ anything	1.5 ± 0.3	0.15 ± 0.03
$pp\to K^{*-}+$ anything	1.2 ± 0.2	0.12 ± 0.02
$\pi^+p\to K^{*+}+$ anything	1.3 ± 0.2	0.16 ± 0.03
$\pi^+p\to K^{*-}+$ anything	0.7 ± 0.2	0.08 ± 0.02
$K^+p\to K^{*+}+$ anything	3.2 ± 1.3	0.27 ± 0.11
$K^+p\to K^{*-}+$ anything	0.6 ± 0.5	0.05 ± 0.04

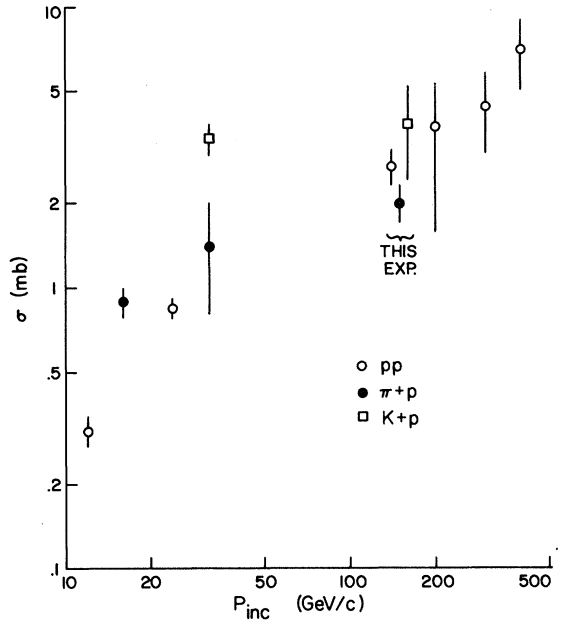

FIG. 7. The total inclusive $K^{*\pm}(890)$ cross section, shown as a function of incident momentum for all three beams used in this experiment.

also a measure of the fraction of $(K^0+\bar{K}^0)$ coming from K^* decay. This ratio is shown in Fig. 8 as a function of beam momentum. It is noteworthy that this ratio shows very little energy dependence; indeed it has about the same value of 0.3 for all three beams over 2 orders of magnitude in energy. Recall that over this energy range the K^0 and K^* cross sections both individually rise sharply,[12] at least for the proton and π^+ beams. These observations are in qualitative agreement with the additive quark model,[10] if most of the strange-particle production is in the central region. In this model, the cross section ratio in the central region is predicted to be independent of the incident particle, because

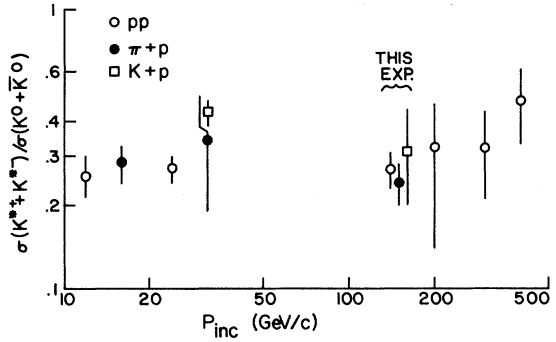

FIG. 8. The ratio of the $K^{*\pm}$ cross section to the K^0 $(\bar{K}^0)$ cross section, shown as a function of incident momentum for all three beams used in this experiment.

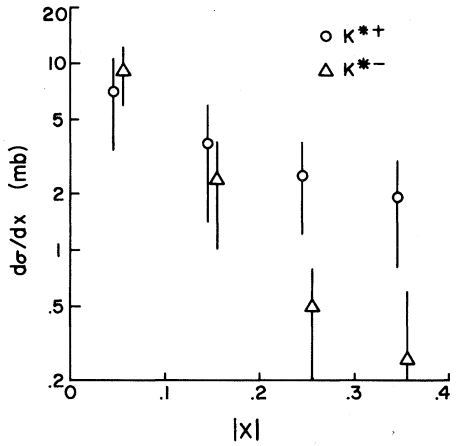

FIG. 9. Feynman-x distributions for K^{*+} and K^{*-} production from the proton beam. The distributions are folded about $x=0$.

the large number of quarks produced do not remember their origin. Such a prediction is also made by the multiperipheral resonance production model.[11]

Finally, we point out that the fundamental importance of resonance production is underscored by the fact that about one-third of the final-state K^0's originate from K^* decay.

IV. INCLUSIVE DISTRIBUTIONS FOR $K^{*\pm}(890)$

We examine next the dependence of $K^*(890)$ production on the Feynman scaling variable x as defined in Sec. I, as well as P_T^2, the square of the transverse momentum. To determine this dependence, we produced $K_S\pi^\pm$ effective-mass distributions in each bin of a particular inclusive variable. These distributions were fitted as described in the previous section to obtain the amount of resonance

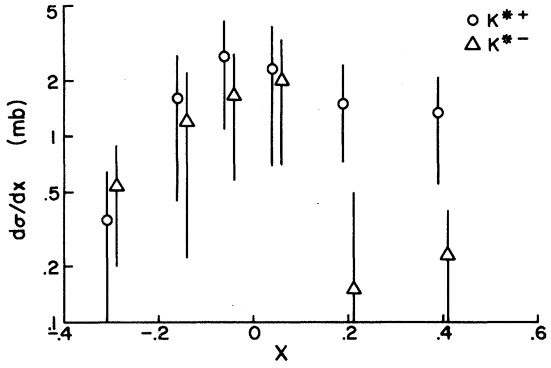

FIG. 10. Feynman-x distributions for K^{*+} and K^{*-} production from the π^+ beam.

production in each bin.

Figure 9 shows the $|x|$ dependence of K^* production by the proton beam in reactions (1) and (2). It is apparent that most of the production is in the central region, where the K^{*+} and K^{*-} cross sections are approximately the same. On the other hand, in the proton fragmentation region there appears to be nonnegligible K^{*+} production, while there is little evidence for K^{*-} production. This observation is in good agreement with the additive quark model.[10] It has also been pointed out[6] that the lack of K^{*-} production in the proton fragmentation region may be attributed to the absence in the proton of either of the valence quarks composing the K^{*-}. Figure 9 is not appreciably affected if we use only the backward hemisphere events in order to avoid the systematic bias against fast, forward K^*. However, the reduction in statistics does increase the errors.

Figure 10 shows the x dependence of K^* production by the π^+ beam in reactions (3) and (4). As in the case of the proton beam, we note an approximate equality of the K^{*+} and K^{*-} cross sections in the central region, followed by an excess of K^{*+} over K^{*-} in the beam fragmentation region. In order to make a rough quantitative measure of this observation, we have chosen $x=0.2$ as a dividing line between the central and beam fragmentation regions, and then calculated the cross-section ratio $\sigma(K^{*-})/\sigma(K^{*+})$ in the two regions for both beams. This ratio is shown in Table III, and does exhibit a marked difference in the two regions. In particular, K^{*-} production is at least four standard deviations less than K^{*+} production in the beam fragmentation region. For completeness, we also show in Table III the cross-section ratio in the target fragmentation region. For the proton beam this region should have the same characteristics as the beam fragmentation region, and indeed the ratio is quite consistent. For the π^+ beam we have very few events in the target fragmentation region, and so the cross-section ratio has a large error.

Transverse-momentum-squared distributions for $K^{*\pm}$ are shown in Figs. 11 and 12 for the proton and π^+ beams, respectively. Experiments at lower energies[2] have found a universal slope of about 3.4

TABLE III. Ratio of K^{*-} to K^{*+} cross sections.

Beam	$\lvert x\rvert < 0.2$	$x > 0.2$	$x < -0.2$
p	1.1±0.4	0.10±0.17	0.21±0.20
π^+	0.7±0.3	0.11±0.14	1.4 ±1.7

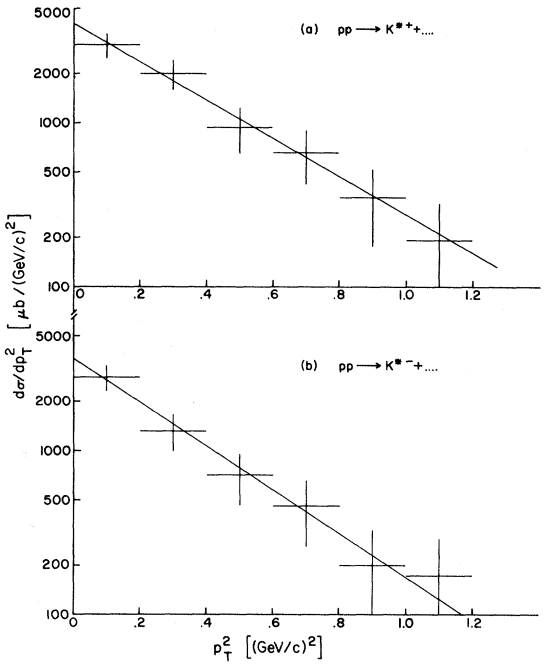

FIG. 11. Transverse-momentum-squared distributions for (a) K^{*+} and (b) K^{*-} from the proton beam. The lines represent exponential fits to the points.

$(\mathrm{GeV}/c)^{-2}$, independent of beam, for particles of mass about 1 GeV. Our values, shown in Table IV, are somewhat lower. However, there is some evidence[1] that all $P_T{}^2$ slopes drop slightly with incident beam energy. To check this, we show in Fig. 13 the variation of the slope with beam energy for K^{*+} and K^{*-} production by proton and π^+ beams. The trend of the data suggests a decrease.

V. INCLUSIVE $Y^{*\pm}(1385)$ PRODUCTION

We used our sample of Λ events to study $Y^{*\pm}$ production in reactions (7)—(12). We followed a procedure analogous to that for the K^* study. The observed Λ's were weighted for geometric detection efficiency, yielding an average escape weight of 1.91. We then examined weighted $\Lambda\pi^+$ and $\Lambda\pi^-$ effective mass distributions from each of the three beams. In general we observed enhancements in

TABLE IV. Fitted $P_T{}^2$ slope parameters in units of $(\mathrm{GeV}/c)^{-2}$.

Beam	K^{*+}	K^{*-}
p	2.7±0.4	3.1±0.5
π^+	2.9±0.4	2.8±0.6

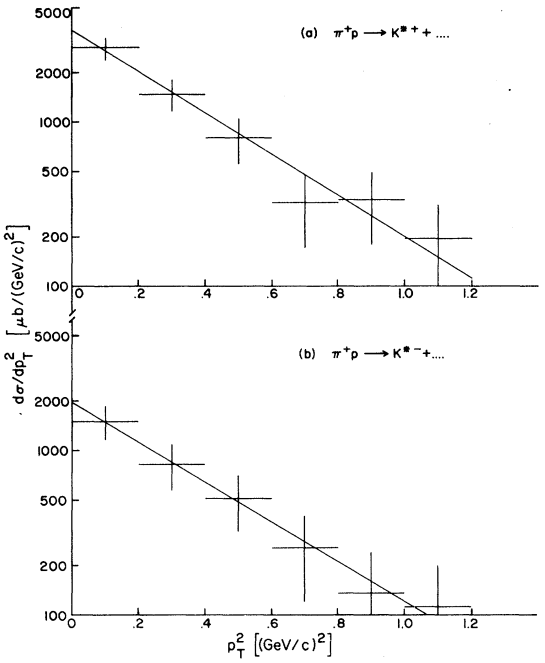

FIG. 12. Transverse-momentum-squared distributions for (a) K^{*+} and (b) K^{*-} from the π^+ beam. The lines represent exponential fits to the points.

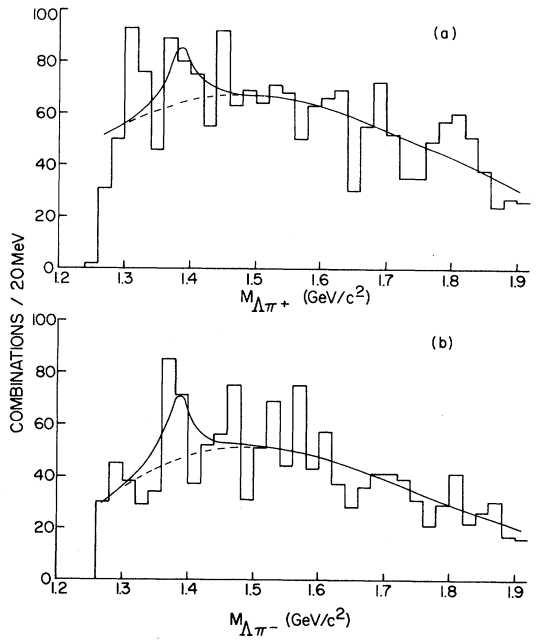

FIG. 14. Escape-weighted effective-mass distributions of (a) $\Lambda\pi^+$ and (b) $\Lambda\pi^-$ for events from the proton beam. The solid line represents a Breit-Wigner fit, while the dashed line represents the background.

the vicinity of the $Y^*(1385)$, but these were less pronounced than the peaks for the K^*.

Figures 14(a) and 14(b) show the escape-weighted $\Lambda\pi^+$ and $\Lambda\pi^-$ mass distributions, respectively, from the proton beam, while Figs. 15(a) and 15(b) show the corresponding distributions from

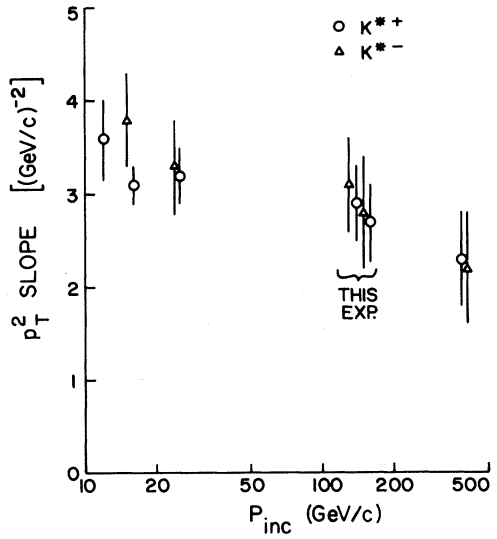

FIG. 13. The slope of the $P_T{}^2$ distributions for K^{*+} and K^{*-}, shown as a function of incident momentum for proton and π^+ beams.

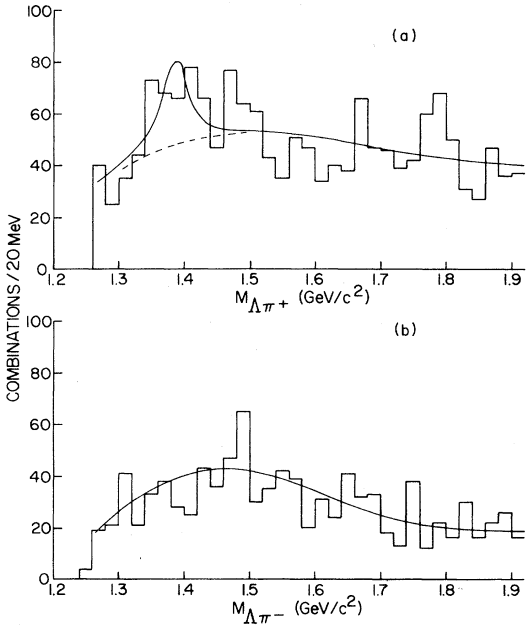

FIG. 15. Escape-weighted effective-mass distributions of (a) $\Lambda\pi^+$ and (b) $\Lambda\pi^-$ for events from the π^+ beam. The solid line represents a Breit-Wigner fit, while the dashed line indicates the background. No evidence for the Y^* was found in (b).

TABLE V. Inclusive cross sections for Y^{*+} and Y^{*-} production. The cross sections are corrected for all unobserved decay modes. Upper limits are quoted at 95% confidence level.

Reaction	σ (mb)	$\sigma(Y^*)/\sigma(\Lambda)$
$pp \to Y^{*+}$ + anything	0.38 ± 0.13	0.09 ± 0.03
$pp \to Y^{*-}$ + anything	0.40 ± 0.13	0.10 ± 0.03
$\pi^+ p \to Y^{*+}$ + anything	0.29 ± 0.07	0.16 ± 0.04
$\pi^+ p \to Y^{*-}$ + anything	< 0.10	< 0.06
$K^+ p \to Y^{*+}$ + anything	0.08 ± 0.18	0.06 ± 0.13
$K^+ p \to Y^{*-}$ + anything	< 0.17	< 0.12

the π^+ beam. Fits to these distributions were made using a smooth polynomial background and a simple Breit-Wigner shape for the Y^*, with a mass of 1385 MeV and a width of 40 MeV. To determine inclusive cross sections, the numbers of escape-weighted events were corrected to account for scan inefficiency, measurement and reconstruction losses, neutral decay modes of the Λ, and the branching ratio of 0.88 for the $Y^{*\pm} \to \Lambda\pi^\pm$ decay.

Table V summarizes the inclusive cross sections for Y^{*+} and Y^{*-} production in reactions (7)–(12). Where upper limits are given, they are at 95% confidence level. For the proton beam the cross sections for the two charge states of the Y^* are very close to each other, suggesting that the production is primarily in the central region. Lower-energy pp experiments[2,3] have observed an excess of Y^{*+} over Y^{*-}, while at higher energies the dominance of central production has been suggested.[6,7]

The approximate equality of the Y^{*+} and Y^{*-} cross sections from the proton beam is observed even if we restrict ourselves to the backward hemisphere and then double the values. We obtain 0.46 ± 0.18 and 0.32 ± 0.14 mb for the Y^{*+} and Y^{*-}, respectively.

By contrast, the meson beams from this experiment do not provide any evidence for Y^{*-} production, while there is a nonnegligible signal for Y^{*+}. This is in agreement with observations at lower energies,[8,9,18] and there are no results above 32 GeV/c with which to compare. If the Y^{*+} is a result of proton fragmentation in the $\pi^+ p$ and $K^+ p$ reactions, it is perhaps surprising that we do not observe an excess of Y^{*+} over Y^{*-} in the pp reactions as well. However, in view of the limited statistics, we certainly cannot rule out some such excess.

Table V also gives the ratio of Y^* to Λ total cross sections. If we assume that Y^* production in pp reactions is primarily in the central region (as suggested by the equality of Y^{*+} and Y^{*-} cross sections) we can make a quantitative test of the additive quark model.[10] This model makes predictions for particle production ratios in the central region. Many of these predictions are dependent on a strange-quark suppression factor λ, whose numerical value is not predicted by the model. Moreover, experimental data have suggested a momentum dependence for λ. However, the Y^*/Λ ratio in the central region is independent of the suppression factor and is predicted to have the value 0.25, both for Y^{*+} and Y^{*-}. Using the fraction of our Λ cross section in the central region[12] and assuming that all the Y^* is central, we obtain $\sigma(Y^{*+})/\sigma(\Lambda) = 0.25 \pm 0.09$ and $\sigma(Y^{*-})/\sigma(\Lambda) = 0.27 \pm 0.09$, which are in excellent agreement with the additive quark model.

ACKNOWLEDGMENTS

This work was supported in part by the U.S. Department of Energy, the National Science Foundation, the U.S.-Israel Binational Science Foundation, and the Dutch Society for Fundamental Research of Matter. We gratefully acknowledge the efforts of the 30-inch bubble-chamber crew, and the scanning and measuring personnel at the participating institutions.

*Present address: Eastern Illinois University, Charleston, Illinois.

†Present address: Dialog Systems, Belmont, Massachusetts.

‡Present address: Universite de Neuchatel, Neuchatel, Switzerland.

§Present address: Stanford Linear Accelerator Center, Stanford, California.

[||]On leave of absence from the Weizmann Institute of Science, Rehovot, Israel.
[¶]On leave of absence from the College de France, Paris, France.
[**]Present address: Tufts University, Medford, Massachusetts.
[††]Present address: Rockefeller University, New York, New York.
[‡‡]Permanent address: Seton Hall University, S. Orange, New Jersey.
[§§]Present address: Fermi National Accelerator Laboratory, Batavia, Illinois.
[|||]Present address: Brookhaven National Laboratory, Upton, New York.

[1]For a recent review, see J. Whitmore, in *Proceedings of the 19th International Conference on High Energy Physics, Tokyo, 1978,* edited by S. Homma, M. Kawaguchi, and H. Miyazawa (Phys. Soc. of Japan, Tokyo, 1979), p. 63.
[2]K. Bockmann *et al.*, Nucl. Phys. B166, 284 (1980); K. Bockmann *et al.*, *ibid.* B143, 395 (1978).
[3]V. Blobel *et al.*, Phys. Lett. 48B, 73 (1974).
[4]R. Singer *et al.*, Nucl Phys. B135, 265 (1978).
[5]F. LoPinto *et al.*, Phys. Rev. D 22, 573 (1980).
[6]H. Kichimi *et al.*, Phys. Rev. D 20, 37 (1979).
[7]H. Kichimi *et al.*, Phys. Lett., 72B, 411 (1978).
[8]I. V. Ajinenko *et al.*, Nucl. Phys. B165, 1 (1980).
[9]P. Granet *et al.*, Nucl. Phys. B140, 389 (1978).
[10]V. V. Anisovich and V. M. Shekhter, Nucl. Phys. B55, 455 (1973).
[11]M. Fukugita *et al.*, Phys. Rev. D 19, 187 (1979).
[12]D. Brick *et al.*, Nucl. Phys. B164, 1 (1980).
[13]D. Brick *et al.*, Phys. Rev. D 21, 632 (1980); M. Schouten *et al.*, Z. Phys. C 9, 93 (1981).
[14]D. Fong *et al.*, Phys. Lett. 53B, 290 (1974).
[15]D. Fong *et al.*, Nucl. Phys. B102, 386 (1976).
[16]Particle Data Group, Rev. Mod. Phys. 52, S162 (1980).
[17]M. Barth *et al.*, Nucl. Phys. B191, 39 (1981).
[18]F. Barreiro *et al.*, Phys. Rev. D 17, 669 (1978).